Published in final edited form as:
Neurotoxicology. 2008 May ; 29(3): 466–470.

Manganese Accumulates Primarily in Nuclei of Cultured Brain Cells

Kiran Kalia[a], **Wendy Jiang**[b], and **Wei Zheng**[b*]

a*School of Biosciences, Sardar Patel University, Vallabh Vidyanagar 388 120, Gujarat, India*

b*School of Health Sciences, Purdue University, West Lafayette, IN 47907, USA*

Abstract

Manganese (Mn) is known to pass across the blood-brain barrier and interact with dopaminergic neurons. However, the knowledge on the subcellular distribution of Mn in these cell types upon exposure to Mn remained incomplete. This study was designed to investigate the subcellular distribution of Mn in blood-brain barrier endothelial RBE4 cells, blood-cerebrospinal fluid barrier choroidal epithelial Z310 cells, mesencephalic dopaminergic neuronal N27 cells, and pheochromocytoma dopaminergic PC12 cells. The cells were incubated with 100 μM $MnCl_2$ with radioactive tracer ^{54}Mn in the culture media for 24 hrs. The subcellular organelles, i.e., nuclei, mitochondria, microsomes, and cytoplasm, were isolated by centrifugation and verified for their authenticity by determining the markers specific to cellular organelles. Data indicated that maximum Mn accumulation was observed in PC12 cells, which was 2.8, 5.2 and 5.9 fold higher than that in N27, Z310 and RBE4 cells, respectively. Within cells, about 92%, 72%, and 52% of intracellular ^{54}Mn were found to be present in nuclei of RBE4, Z310, and N27 cells, respectively. The recovery of ^{54}Mn in nuclei and cytoplasm of PC12 cells were 27% and 69% respectively. Surprisingly, less than 0.5% and 2.5% of cellular ^{54}Mn was found in mitochondrial and microsomal fractions, respectively. This study suggests that the nuclei may serve as the primary pool for intracellular Mn; mitochondria and microsomes may play an insignificant role in Mn subcellular distribution.

Keywords

Manganese; Nuclear fraction; Mitochondria; Z310 cells; RBE4 cells; PC12 cells; N27 cells

1. Introduction

Neurotoxicity due to excessive manganese (Mn) accumulation in specific brain area produces symptoms resembling those of idiopathic Parkinson's disease (IPD). The mechanism by which Mn causes the neurodegenerative damage is not clearly understood. As an essential element, Mn plays a vital role for normal development and body functions across the life span of all mammals (Keen et al., 2000). In brain about 80% of Mn is associated with the astrocyte specific enzyme glutamine synthase (Wedler and Denman, 1984). Excessive levels of brain Mn has

*__To Whom the Correspondence Should be Addressed:__ Dr. Wei Zheng, Ph.D., Purdue University School of Health Sciences, 550 Stadium Mall Drive, CIVL 1163D, West Lafayette, IN 47907, Phone: 765-496-6447, Fax: 765-496-1377, E-mail: wzheng@purdue.edu.

been linked to the loss of dopamine in the striatum, death of non-dopaminergic neurons in the globus pallidus, and damage of other neuronal pathways such as glutamate and γ-amino butyrate (GABA), all of which contribute to altered behavior, motor dysfunction and cognition deficit (Aschner et al., 2002, Dorman et al., 2000, Erikson et al., 2002, Montes et al., 2001, Takeda et al., 2002).

Mn concentration in serum is about 0.05–0.12 μg/dL in healthy individuals. After exposure, Mn readily distributes into other tissues. Previous data from this laboratory using animal models suggest that under normal conditions Mn distributes in brain in the following order: substantia nigra > striatum > hippocampus > frontal cortex in a concentration range of 0.03–0.07 μg/g wet tissue weight (Zheng et al., 1998). Mn readily enters the brain via three known pathways, i.e., through the capillary endothelial cells of the blood-brain barrier (BBB), by the choroidal epithelial cells of the blood-cerebrospinal fluid (CSF) barrier, or via the olfactory nerve from the nasal cavity directly to brain (Aschner et al., 2007). The tight junction structure, located between capillary endothelial cells of the BBB, inhibits the movement of substances between the blood and brain parenchyma. The choroid plexus, which produces about 90% of the CSF within brain ventricles, constitutes the blood–CSF barrier (BCB) with the tight junctions between epithelial cells. At near physiological plasma concentration (80 nM Mn or 4.4 ng/mL), brain influx of Mn was reported primarily through the capillary endothelium of the BBB, while at the higher concentration (78 μM or 4.28 μg/mL), the influx of Mn was primarily via the BCB to the CSF (Murphy et al., 1991, Rabin et al., 1993).

Mn is known to pass across the brain barrier and accumulate in specific brain areas. However, much less is known about intracellular distribution of Mn in brain cells following exposure. Liccione and Maines (1988) suggest that upon entering the cells, Mn mainly accumulates in mitochondria. Gavin et al. (1999) further indicate that a slow efflux of Mn by mitochondria accounts for the excess accumulation of Mn ions in this subcellular organelle. Additional reports demonstrate an accumulation of Mn in mitochondria where Mn^{2+} may be oxidized to Mn^{3+} (Archibald and Tyree, 1987; Gunter et al., 2004, 2006). Surprisingly, there has been no direct evidence in literature on subcellular distribution of Mn.

Mn exposure causes cellular oxidative damage and inhibits oxidative phosphorylation in brain cells (Gavin et al., 1992). Different brain cells exhibit different sensitivity to Mn toxicity; astrocytes sequester more Mn than neurons and thus may have higher tolerance to Mn toxicity than neurons (Zwingmann et al., 2003). To explore the mechanism of Mn neurotoxicity and identify the potential susceptibility of cell types to Mn exposure, it is necessary to have thorough understanding of the intracellular distribution of Mn within different types of brain cells. In our recent attempt to explore the mechanism of para-aminosalicylic acid (PAS) in effective treatment of manganism patients (Jiang et al., 2006), there is a need to study whether and how this drug may mobilize the intracellular pool of Mn. Thus, the purpose of this study was to determine and compare the subcellular distribution of Mn in cell types that are important for Mn transport and toxicity. We chose choroidal epithelial Z310 cells established from the choroid plexus of the BCB (Zheng and Zhao, 2002), brain endothelium RBE4 cells derived from rat brain endothelium of the BBB (Roux et al., 1994), mesencephalic dopaminergic neuronal (N27) cells (Prasad et al., 1994), and pheochromocytoma PC12 cells derived from rat adrenal medulla (Greene and Tischler, 1976), for this study.

2. Materials and Methods

2.1. Cell culture

Choroidal Z310 cells were cultured in Dulbecco's modified eagle's medium(DMEM) (Invitrogen, Carlsbad, CA) supplemented with 10% fetal bovine serum (FBS) (Zheng and Zhao, 2002). Brain endothelial RBE4 cells were grown in collagen-coated flasks in a minimum

essential medium/Ham's F10 (1:1, v/v; Invitrogen) supplemented with 2 mM glutamine, 10% FBS, and 1 ng/mL basic fibroblast growth factor according to the method described by Aschner et al. (2002). Dopaminergic N27 cell were cultured in RPMI 1640 medium with 100 units of penicillin, 100μg/ml streptomycin and 10% fetal calf serum (Invitrogen) by the method described by Prasad et al. (1994). PC12 cells were cultured in lysine-coated plates in RPMI 1640 medium supplemented with 10% heat-inactivated horse serum and 5% FBS. Cells were maintained in a humidified incubator with 95% air-5% CO_2 at 37°C. The cultures that reached the half confluence (usually within 4–6 days) were used for the experiments described below.

2.2. Mn exposure and preparation of subcellular fractions

A Mn solution was prepared by dissolving $MnCl_2$ in distilled ,deionized water at a concentration of 40 mM, which was autoclaved prior to the use. An aliquot (1 mL) of this solution was mixed with a pre-diluted $^{54}MnCl_2$ solution (specific activity 7.734 Ci/mL, Perkin Elmer, Waltham, MA) to yield a hot solution containing 1.053 μCi ^{54}Mn. An aliquot (25 μL) of this hot solution was then added per 10 mL culture medium for Mn treatment. The half confluent cultures of Z310, RBE4, N27, or PC12 cells were exposed to 100 μM $MnCl_2$ containing 2.633 nCi ^{54}Mn/mL for 24 hrs. The exposure concentration was chosen because previous works by this and other laboratories have shown significant toxic outcomes in various cell types (Chen et al., 2001; Crooks et al., 2007; Gunter et al., 2006; Li et al., 2005; Zheng and Zhao, 2001). Mn treatment was terminated by rapid aspiration of the medium, followed by thorough washes with 5 mL of ice cold PBS for three times.

To prepare subcellular fractions, cells from five 10-cm^2 plates (for Z310, N27 or PC12) or five 75-cm^2 flasks (for RBE4) were used. Z310 and RBE4 cells were scrubbed off following incubation in 0.3 mL of 0.25% trypsin at 37 °C for 10 and 3 min, respectively, and neutralized with 1.7 mL of the respective culture media. N27 and PC12 cells were scrubbed off using a rubber policeman in 2.0 mL ice-cold PBS and cells were centrifuged at 800 × g for 10 min at 4°C. The cell pellet was further fractionated to separate nuclear and mitochondrial fractions using the Mitochondria Isolation kit (Pierce, Rockford, IL) according to the Instruction of the assay kit. The post-mitochondrial supernatant was further ultra-centrifuged at 100,000 × g for 60 min for separation of microsomes (pellet) and cytoplasm (supernatant).

For preparation of "pure" nuclear fraction, cells from five parallel sets of plates/flasks were treated with Nuclei Pure-Prep nuclei isolation kit (Sigma). The cells were scrubbed off using a rubber policeman in 10 mL of ice-cold lysis buffer containing 1.0 mM freshly prepared DTT and 0.01% triton X-100 and then transferred to centrifuge tubes. The pure nuclei fraction was obtained by centrifugation at 38,000 g × 90 min (Beckman coulter - Avanti J-251 centrifuge using SWi41Ti rotor) through a dense sucrose cushion, which protects nuclei and removes cytoplasmic contaminants as suggested in the Instruction of the assay kit.

Cells from one another parallel plate/flask were collected and counted after trypan-blue staining and used for total cellular ^{54}Mn uptake studies.

2.3. Protein separation and verification of subcellular fractions

To prepare the protein fractions for further analyses, cells along with their subcellular fractions were disrupted using celLytic MT Mammalian Tissue Lysis/Extraction buffer (Sigma) and by sonication (VWR Sonifer Model 250) at a setting of 20% output and 3.5 control for 20 pulses. The protein fractions were subjected to counting of radioactivity or frozen at −80 °C for protein determination or Western blot analysis.

The authenticity of subcellular fractions was confirmed by Western blot analysis as previously described by (Ke et al., 2003), using primary monoclonal antibodies anti-nuclear core complex

proteins-clone4 for nuclear fraction, anti-cytochrom-c oxidase for mitochondria, and anti-lactate dehydrogenase (H-subunit of LDH) clone HH-17 for cytoplasmic fraction (all were purchased from Sigma). A volume of protein extracts (40 μg) of total cell lysate, nuclei, mitochondria or cytoplasm was mixed with an equal volume of 2x sample buffer (0.125M Tris, 4% SDS, 20% glycerol, 0.02% 2-mercaptoethanol, and 0.01% bromophenol Blue), electrophoresed on a 4 –20% Tris–HCl linear gradient ready gels (Bio-Rad, Hercules, CA), and transferred to a PVDF membrane. The membranes were blocked with 5% dry milk in TBS-T (Tris buffered saline with 0.1% Tween-20) and then incubated with 1:500 aforementioned primary antibodies. After three washes with TBS-T, the membranes were further treated with the HRP-conjugate goat anti mouse IGg1 antibody (1:2000) for nuclear pore protein and lactate dehydrogenase and an HRP-conjugated donkey anti sheep antibody (1:5000) for mitochondrial cytochrome- c oxidase. The membranes were developed using enhanced chemiluminescence (ECL, GE Healthcare, Piscataway, NJ). The band intensity was quantified using UN-SCAN-IT tm V5.1 software (Silk Scientific Inc. Orem, UT).

Total and subcellular fraction protein concentrations were assayed by Bradford protein assay (Bradford, 1976). ^{54}Mn radioactivity was counted using a Packard model Cobra-II gamma counter.

2.4. Statistical analysis

All values are expressed as mean ± S.D. The replicates of experiments conducted on the same day were referred as n=1; three or four such replicates on different dates were used for statistical analyses by one way (ANOVA) F-test followed by Dunnet (2-sided) or Tukey HSD-test using SPSS-10 software. The statistical significance was considered when p – value was less than 0.05.

3. Results and Discussion

Following exposure of the cells to Mn at 100 μM, the maximum Mn accumulation was observed in PC12 cells, which was 2.8, 5.2 and 5.9 fold higher than that in N27, Z310 and RBE4 cells, respectively (Fig. 1). The amount of Mn in N27 cells was about 1.6 and 1.8 fold more than those of Z310 and RBE4. These data revealed that neuronal cells such as PC12and N27 cells appeared to have a much higher capacity in accumulating Mn ions from the culture medium than non-neuronal cells that constitute the BBB (endothelial RBE4) and the BCB (epithelial Z310). As the barrier cells, both RBE4 and Z310 cells possess metal transporters such as divalent metal transporter (DMT1) and transferrin receptor (TfR), which facilitate the uptake of Mn into the cells. Both barrier cells also express metal transport protein (MTP1) whose function is to expel the metal from the cells to surrounding environment (Burdo et al., 2001). The active influx and efflux capacities render the Z310 and RBE4 cells not only effective in taking up Mn but also capable of dispersing the metal to surrounding medium. Dopaminergic cell type such as PC12 cells also express DMT1 and TfR (Loder and Melikian, 2003;Roth et al., 2002). However, the presence of metal exporter protein MTP1 in PC12 or N27 cells is unknown. It is possible that a tight metal intracellular binding and/or a weak efflux of metals in these two cell lines may contribute to a high accumulation of Mn in these cells. This possibility, however, waits for further experimental corroboration.

A primary goal of this study was to investigate the subcellular distribution of Mn. It is therefore critical to ensure that the prepared fractions are indeed the ones representative of subcellular organelles studied. Western blot analyses of protein markers for each subcellular fraction revealed that the nuclear core complex protein, cytochrome-c oxidase, and LDH H-chain protein were strongly expressed in the nuclear, mitochondrial and cytoplasmic fraction, respectively, but weakly or not present at all in other subcellular fractions in respective samples

(Fig. 2). The data confirmed that the method we used was able to separate the cellular organelles for investigating subcellular distribution of Mn.

Counting ^{54}Mn radioactivity in each subcellular fraction indicated that there was no significant loss of ^{54}Mn during the subcellular fractionation. Most of the Mn ions accumulated in the nuclei; the phenomenon was true for all tested cell types (Fig. 3A). If the total cellular ^{54}Mn radioactivity was accounted for 100%, about 92% and 72% of intracellular ^{54}Mn were found to be present in nuclei of RBE4 and Z310 cells, respectively. N27 cells had 52% and 35% of Mn found in nuclei and cytoplasm, respectively. Interestingly, while the nuclei of PC12 cells possessed a significant amount (27%) of ^{54}Mn, the majority (69%) of ^{54}Mn was recovered from the cytoplasm. Far to our surprise, however, less than 0.5% of cellular ^{54}Mn was recovered from mitochondrial fractions of all 4 tested cell lines (Fig. 3A). The ^{54}Mn recovered from the microsomal fractions were less than 2.5% among tested cells. Thus, it appeared unlikely that mitochondria and microsomes were the major pools in intracellular Mn storage.

It is possible that Mn may be protein-bound; the less protein amount in a particular cellular organelle may result in a less accumulation of Mn. We therefore determined the protein concentrations in each subcellular fraction. Fig. 3B depicts that when the ^{54}Mn counts were justified by protein amounts, the nuclear fraction of Z310 and RBE4 cells contained the highest amount of ^{54}Mn per mg protein, whereas the highest amounts of ^{54}Mn were recovered from cytoplasmic proteins, followed by nuclear proteins, in N27 and PC12 cells. Again, the mitochondrial proteins contained insignificant amounts of ^{54}Mn.

To further confirm the Mn accumulation in the nucleus, we used the dense sucrose cushion followed by density-gradient centrifugation to prepare pure nuclei pellets from 4 tested cell lines. The results were then compared to the ^{54}Mn distribution data from partially purified nuclei. Results in Fig. 4 indicated that there was no significant difference in nuclear accumulation of ^{54}Mn between two methods for nuclear fraction preparation.

Our current study contradicts most of the previous studies where Mn is shown to be mainly sequestered by mitochondria (Gavin et al. 1999; Gunter and Puskin 1972, Liccione and Maines 1988). One possible explanation pertains to experimental design. For example, the study by Liccione and Maines (1988) determined the activities of mitochondrial GSH-peroxidase, catalase, and gamma-glutamyltranspeptidase, but it did not measure Mn concentrations in mitochondria or cytosol. Other Mn studies with mitochondria are essentially to use mitochondrial preparations for the purpose of studying Mn uptake and efflux kinetics (Gunter and Puskin 1972; Gavin et al., 1999), interaction with Ca^{2+} uniporter (Gavin et al., 1992), and speciation catalyzed by isolated mitochondrial preparations (Gunter et al., 2004). The present study, however, directly determined ^{54}Mn in relatively well-isolated subcellular fractions. Noticeably, a recent report by Morello and colleagues (2007) has also come to the similar conclusion that specific nuclear components in neurons and astrocytes may represent the preferential targets for Mn accumulation and toxicity. It should be pointed out that a relatively small amounts of Mn in the mitochondrial fraction as demonstrated by this and Morello's work should not rule out the importance of mitochondria in Mn-induced cytotoxicity, as the structural and functional integrity of mitochondria is pivotal to the cell survival.

Why does the nucleus have such a high capacity in accumulating Mn? Currently we do not have a good explanation with sound experimental evidence. The ability of Mn to interact with nucleotides of DNA, RNA and ribosomes has been demonstrated by in vitro experiments (Jouve et al., 1975; Pan et al., 1993; Vogtherr and Limmer, 1998). We believe, however, that Pirin, a highly conserved nuclear protein that is exclusively localized within the nucleoplasma and predominantly concentrated within dot-like sub-nuclear structures, may play a role. This newly identified protein has the Fe^{2+} binding site, closely resembles that found in Germin, a

Mn-containing protein (Pang et al., 2004). The highly conserved metal binding site in the N-terminal β-barrel of Pirin may allow Mn to replace Fe and therefore offer a depot for Mn ions in nuclei. Aside Pirin, there may be other yet unidentified nuclear proteins targeted by Mn. These interesting hypotheses deserve further investigation.

In summary, the current study indicates that upon Mn exposure, most of Mn ions tend to accumulate in nuclei of Z310 and RBE4 cells. In dopaminergic N27 and PC12 cells, significant portions of Mn accumulate in both nuclear and cytoplasmic fractions. Overall, the mitochondria and microsomes possess minor amounts of cellular Mn.

Acknowledgment

Prof. Kalia is thankful to Department of Biotechnology, Government of India, to support this study under Overseas Research Associateship Programme. This work was supported in part by NIH/National Institute of Environmental Health Sciences grant ES08164 and ES013118.

References

Archibald F, Tyree C. Manganese poisoning and the attack of trivalent manganese upon catacholamines. Arch Biochem Biophys 1987;256:638–650. [PubMed: 3039917]

Aschner M, Nass R, Guilarte TR, Schneider JS, Zheng W. Manganese neurotoxicity: From worms to men. Toxicol Appl Pharmacol 2007;221:131–147. [PubMed: 17466353]

Aschner M, Shanker G, Erikson K, Yang J, Mutkus LA. The uptake of manganese in brain endothelial cultures. Neurotoxicology 2002;23:165–168. [PubMed: 12224757]

Bradford MM. A rapid and sensitive method for the quantification of microgram quantities of protein utilizing the principle of protein-dye binding. Anal Biochem 1976;72:248–254. [PubMed: 942051]

Burdo JR, Menzies SL, Simpson IA, Garrick LM, Garrick MD, Dolan KG, Haile DJ, Beard JL, Connor JR. Distribution of divalent metal transporter 1 and metal transport protein 1 in the normal and Belgrade rat. J Neurosci Res 2001;66:1198–1207. [PubMed: 11746453]

Chen JY, Tsao G, Zhao Q, Zheng W. Differential cytotoxicity of Mn(II) and Mn(III): special reference to mitochondrial [Fe-S] containing enzymes. Toxicol Appl Pharmacol 2001;175:160–168. [PubMed: 11543648]

Crooks DR, Welch N, Smith DR. Low-level manganese exposure alters glutamate metabolism in GABAergic AF5 cells. Neurotoxicology 2007;28:548–554. [PubMed: 17320182]

Dorman DC, Struve MF, Vitarella D, Byerly FL, Goetz J, Miller R. Neurotoxicity of manganese chloride in neonatal and adult DC rat following subchronic (21 days) high-dose oral exporsure. J Appl Toxicol 2000;20:179–187. [PubMed: 10797470]

Erikson K, Shihabi Z, Aschner J, Aschner M. Manganese accumulates in iron deficient rat brain regions in a heterogeneous fashion and is associated with neurochemical alterations. Biol Trace Elem Res 2002;87:143–156. [PubMed: 12117224]

Gavin CE, Gunter KK, Gunter TE. Mn^{2+} sequestration by mitochondria and inhibition of oxidative Phosphorylation. Toxicol Appl Pharmacol 1992;115:1–5. [PubMed: 1631887]

Gavin CE, Gunter KK, Gunter TE. Manganese and calcium transport in mitochondria: implications for manganese toxicity. Neurotoxicology 1999;20:445–454. [PubMed: 10385903]

Gunter KK, Aschner M, Miller LM, Eliseev R, Salter J, Anderson K, Gunter TE. Determining the oxidation states of manganese in NT2 cells and cultured astrocytes. Neurobiol Aging 2006;27:1816–1826. [PubMed: 16290323]

Gunter T, Gavin CE, Aschner M, Gunter KK. Speciation of manganese in cells and mitochondria: A search for the proximal cause of manganese neurotoxicity. Neurotoxicology 2006;27:765–776. [PubMed: 16765446]

Gunter T, Miller L, Gavin C, Eliseev R, Salter J, Buntinas L, Alexandrov A, Hammond S, Gunterx K. Determination of the oxidation states of manganese in brain, liver, and heart mitochondria. J Neurochem 2004;88:266–280. [PubMed: 14690515]

Gunter T, Puskin J. Manganese ion as a spin label in studies of mitochondrial uptake of manganese. Biosphys J 1972;12:625–635.

Greene LA, Tischler AS. Establishment of a noradrenergic clonal line of rat adrenal pheochromocytoma cells which respond to nerve growth factor. Proc Natl Acad Sci USA 1976;73:2424–2428. [PubMed: 1065897]

Jiang YM, Mo XA, Du FQ, Fu X, Zhu XY, Gao HY, Xie JL, Liao FL, Pira E, Zheng W. Effective Treatment of Manganese-Induced Occupational Parkinsonism with PAS-Na: A Case of 17-Year Follow-Up Study. J Occup Env Med 2006;48:644–649. [PubMed: 16766929]

Jouve H, Jouve H, Melgar E, Lizarrage B. Astudy of the bnding of Mn2+ to bovine pancreatic deoxyribonuclease I and to deoxyribonucleic acid by paramagnetic resonance. J Biol Chem 1975;250:6631–6635. [PubMed: 169255]

Ke Y, Chen Y, Chang Y, Duan X, Ho K, Jiang H, Wang K, Qian Z. Post-transcriptional expression of DMT1 in the heart of rat. J Cell Physiol 2003;196:124–130. [PubMed: 12767048]

Keen, CL.; Ensunsa, J.; Clegg, M. Manganese metabolism in animals and humans including the toxicity of manganese. In: Sigel, A.; Sigle, H., editors. Manganese and its Role in Biological Processes. New York: Marcel Dekker; 2000. p. 89-121.

Li GJ, Zhao Q, Zheng W. Alteration at translational but not transcriptional level of transferrin receptor expression following manganese exposure at the blood-CSF barrier in vitro. Toxicol Appl Pharmacol 2005;205:188–200. [PubMed: 15893546]

Liccione J, Maines M. Selective vulnerability of glutathione metabolism and cellular defense mechanisms in rat striatum to manganese. J Pharmacol Exp Ther 1988;247:156–161. [PubMed: 2902211]

Loder MK, Melikian HE. The dopamine transporter constitutively internalizes and recycles in a protein kinase C-regulated manner in stably transfected PC12 cell lines. J Biol Chem 2003;278:22168–22174. [PubMed: 12682063]

Montes S, Alcaraz-Zubeldia M, Muriel P, Riosv C. Striatal manganese accumulation induces changes in dopamine metabolism in cirrhotic rats. Brain Res 2001;891:123–129. [PubMed: 11164815]

Morello M, Canini A, Matioli P, Sorge RP, Alimonti A, Bocca B, Forte G, Martorana A, Bernardi G, Sancesario G. Sub-cellular localization of manganese in the basal ganglia of normal and manganese-treated rats An electron spectroscopy imaging and electron energy-loss spectroscopy study. NeuroToxicology 2008;29:60–72. [PubMed: 17936361]

Murphy V, Wadhwani K, Smith Q, Rapoport S. Saturable transport of manganese(II) across the rat blood-brain barrier. J Neurochem 1991;57:948–954. [PubMed: 1861159]

Pan, T.; Long, DM.; Uhlenbeck, OC. Divalent metal ions in RNA folding and catalysis. In: Gestland, RF.; Atkins, JF., editors. The RNA World Gestland. New York: Cold Spring Harbor Laboratory Press; 1993. p. 271-302.

Pang H, Bartlam Q, Zeng H, Miyatake T, Hisano K, Miki L, Wong G, Gao F, Rao Z. Crystal structure of human pirin: an iron-binding nuclear protein and transcription cofactor. J Biol Chem 2004;279:1491–1498. [PubMed: 14573596]

Prasad KN, Carvalho1 E, Kentroti S, Edwards-Prasad J, Freed C, Vernadakis A. Establishment and characterization of immortalized clonal cell lines from fetal rat mesencephalic tissue. In Vitro Cell Dev Biol – Animal 1994;30:596–603.

Rabin O, Hegedus L, Bourre JM, Smith QR. Rapid brain uptake of manganese (II) across the blood-brain barrier. J Neurochem 1993;61:509–517. [PubMed: 7687654]

Roth JA, Horbinski C, Higgins D, Lein P, Garrick MD. Mechanisms of manganese-induced rat pheochromocytoma (PC12) cell death and cell differentiation. Neurotoxicology 2002;23:147–157. [PubMed: 12224755]

Roux F, Durieu-Trautmann O, Chaverot N, Claire M, Mailly P, Bourre JM, Strosberg AD, Couraud PO. Regulation of gamma-glutamyl transpeptidase and alkaline phosphatase activities in immortalized rat brain microvessel endothelial cells. J Cell Physiol 1994;159:101–113. [PubMed: 7908023]

Takeda A, Takatsuka K, Sotogaku N, Oku N. Influence of iron-saturation of plasma transferring in iron distribution in the brain. Neurochem Int 2002;41:223–228. [PubMed: 12106773]

Vogtherr M, limmer S. NMR study on the impact of metal ion binding and deoxynucleotide substitution upon local structure and stability of small ribozyme. FEBS Lett 1998;433:301–306. [PubMed: 9744815]

Wedler FC, Denman R. Glutamine synthase: the major Mn(II) enzyme in mammalian brain. Curr Top Cell Regul 1984;24:153–169. [PubMed: 6149889]

Zheng W, Ren S, Graziano J. Manganese inhibits mitochondrial aconitase: a mechanism of manganese neurotoxicity. Brain Res 1998;799:334–342. [PubMed: 9675333]

Zheng W, Zhao Q. Iron overload following manganese exposure in cultured neuronal, but not neuroglial cells. Brain Res 2001;897:175–179. [PubMed: 11282372]

Zheng W, Zhao Q. Establishment and characterization of an immortalized Z310 choroidal epithelial cell line from murine choroids plexus. Brain Res 2002;958:371–380. [PubMed: 12470873]

Zwingmann C, Leidfritz D, Hazel AS. Energy metabolism in astrocytes and neurons treated with manganese: Relation among cell-specific energy failure, glucose metabolism, and intracellular trafficking using multinuclear NMR-spectroscopin analysis. J Cereb Blood Flow Metab 2003;23:756–771. [PubMed: 12796724]

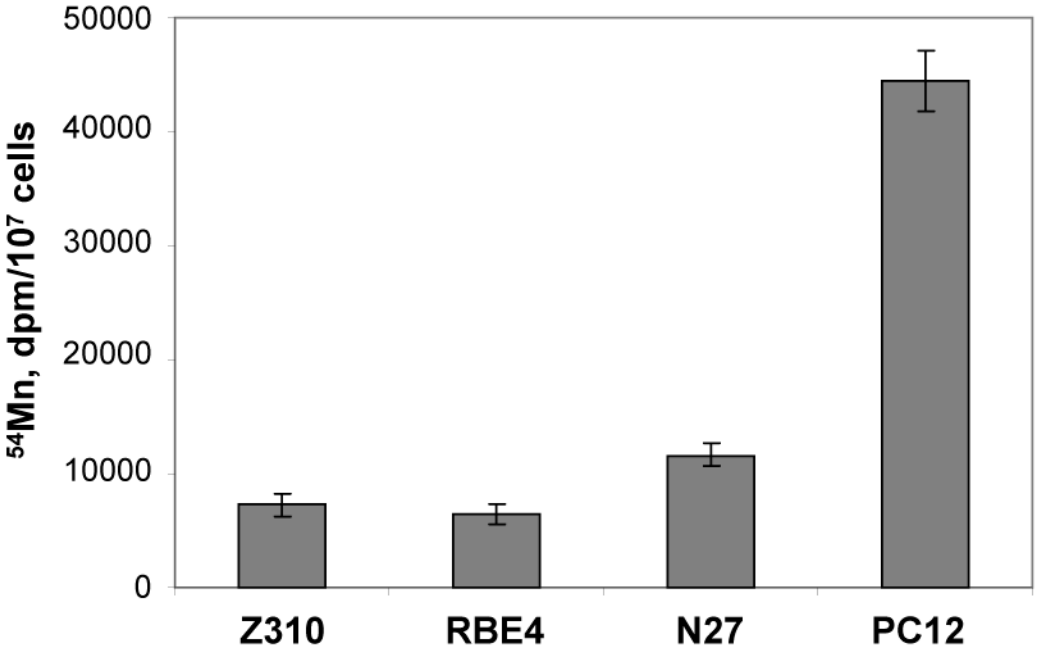

Fig. 1. Total Mn Uptake by Various Cell Types

Total Mn uptake by various cell types. Cells were treated with 100 μM Mn (with 2.63 nCi ^{54}Mn) for 24 hr. Cells were thoroughly washed, collected and counted for radioactivity. Data represent mean ± S.D., n=4. $p<0.001$ compared among each other excerpt for between Z310 and RBE4 groups.

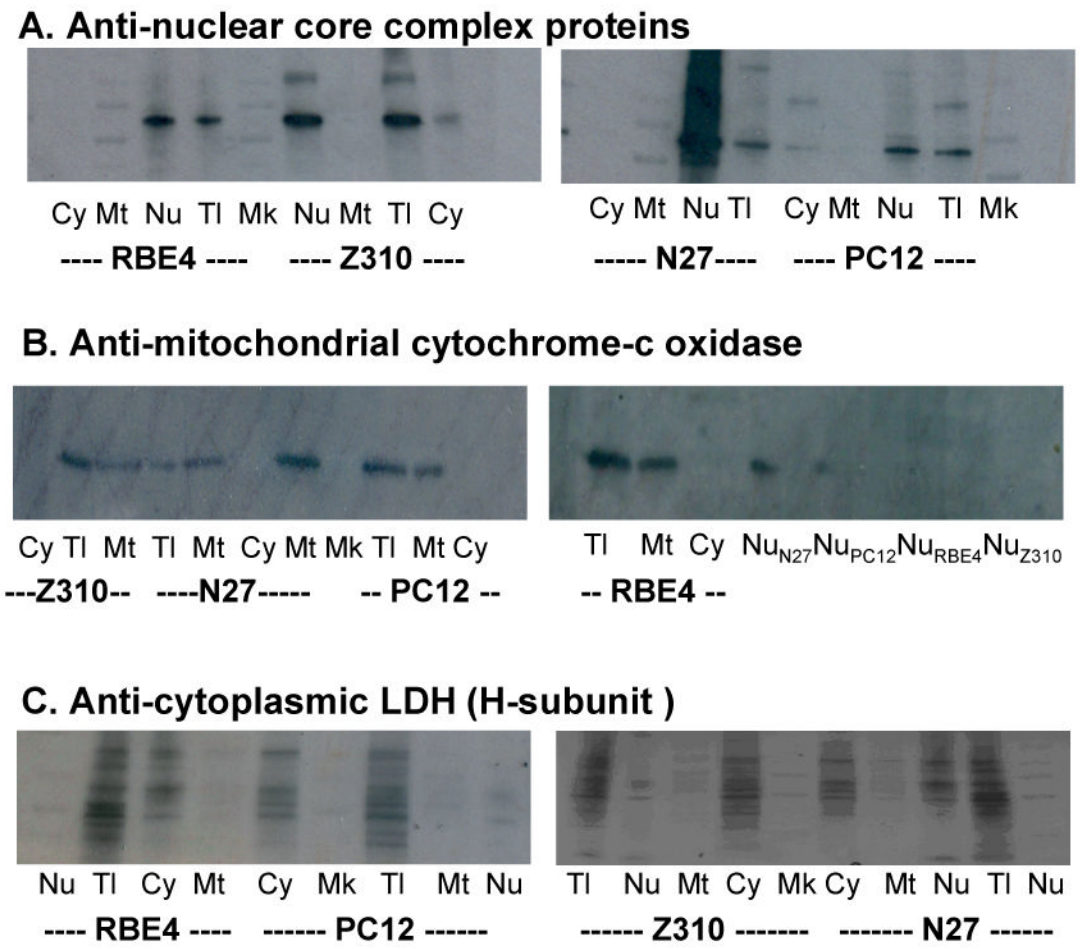

Fig. 2. Verification of Subcellular Fractions

Verification of subcellular fractions by Western blot analysis. Cells were processed to obtain various subcellular fractions (See the main text for details), followed by preparation of cellular proteins. A sample of 40 μg proteins was applied to each lane. (A). Using anti-nuclear core complex protein antibody to verify the nucleus fraction. (B). Using anti-cytochrome c oxidase antibody to verify the mitochondrial fraction. (C). Using anti-LDH heavy chain antibody to verify cytoplasmic fraction. Cy, cytoplasm; Mt, mitochondrion; Nu, nucleon; Tl, total cellular protein; and Mk, marker protein.

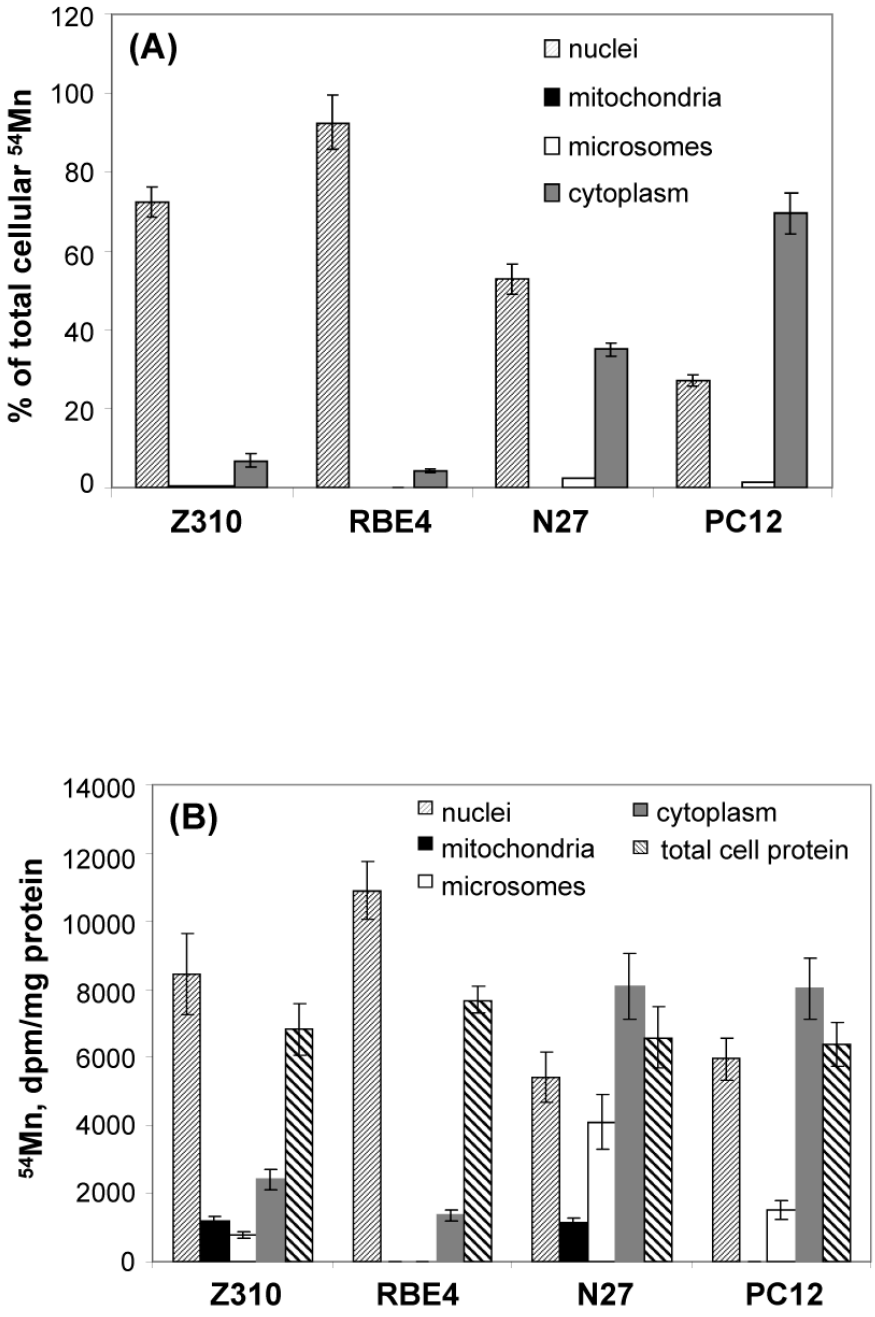

Fig. 3. Fig. 3A. Subcellular Distribution of ^{54}Mn (% of Total ^{54}Mn). Fig. 3B. Subcellular Distribution of ^{54}Mn (per mg Protein)

Subcellular distribution of Mn following Mn exposure. Cells were treated with 100 μM Mn (with 2.63 nCi ^{54}Mn) for 24 hr. (A). The subcellular fractions were isolated and counted for radioactivity as the % of the total cellular Mn. Within group, the % in nuclei was significantly different from those in other subcellular preparation ($p<0.001$). Between groups, the % in nuclei were significantly different from one group from another ($p<0.05$); the % in cytoplasm were also significantly different from each other ($p<0.05$) except for % between Z310 and RBE4. (B). The subcellular fractions were isolated. In addition to determination of radioactivity, each

fraction was subjected to protein assay and expressed as dpm per mg of protein. Data represent mean ± S.D.

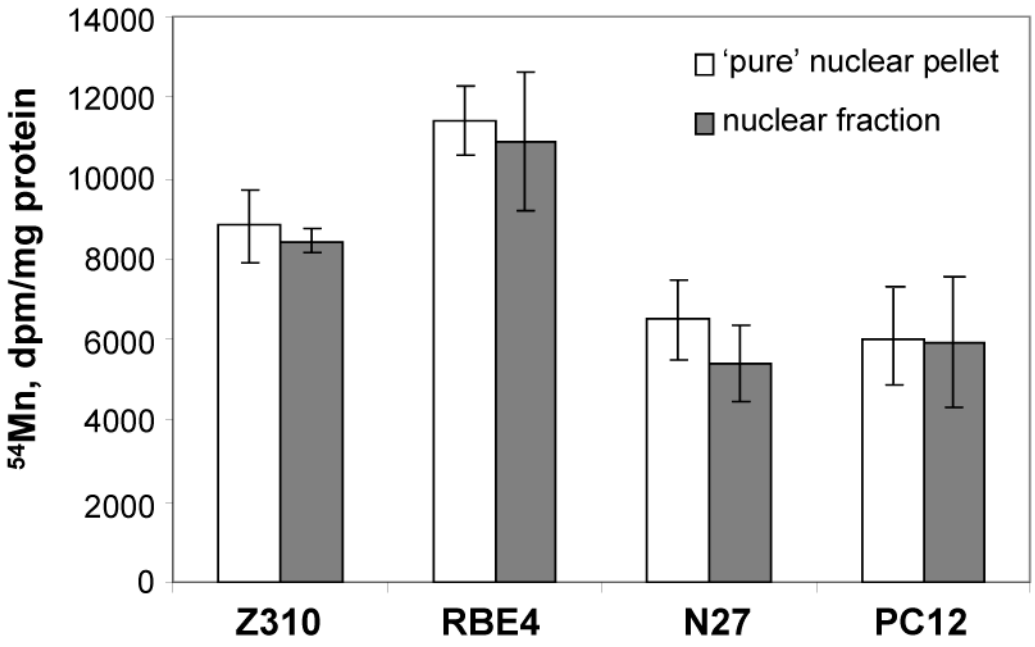

Fig. 4. Nuclear Distribution of ^{54}Mn by Different Method

Comparison of Mn accumulation in nuclear pellet separated by different "methods". The nuclear fraction was prepared by centrifugation. The pure nuclear pellet was prepared using the dense sucrose cushion followed by density-gradient centrifugation. Data represent mean ± S.D., n=4.

Table 1

Percent recovery of ^{54}Mn in each cellular fraction of different types of brain cell lines

No of cells	Z310 (8.5 ×10^7)		RBE4 (7.1 ×10^7)		N27 (4.1×10^7)		PC12 (3.3×10^7)	
	dpm	% recovered	dpm	% recovered	dpm	% recovered	Dpm	% recovered
Total cell suspension	61106±7170		45536±3796		47051±3150		144031 ±14084	
nuclear fraction	44413±1869	72.7	42171±1728	92.6	24897±1260	52.9	39453±4067	27.4
mitochondrial fraction	189±38	0.31	0±0		69±3	0.14	0±	
microsomal fraction	275±24	0.45	0±0		1166±52	2.4	1827±311	1.26
cytosolic fraction	4209±66	6.88	2000±72	4.39	16479±736	35.0	99820±11251	69.3

Data represent mean ± SD, n=4.